Ion-gating Synaptic Memristor Based On Tri-layer HfO_x Composition Regulation

Lanqing Zou[1], Junming Zhang[1], Yunhui Yi[1], Jiawang Ren[1], Huajun Sun[1,2*], Chuqian Zhu[1], Jiyang Xu[1], Sheng Hu[1,3], Lei Ye[1,2], Weiming Cheng[1,2], Qiang He[1,2], Xiangshui Miao[1,2]

AFFILIATIONS

[1]School of Integrated Circuits, Hubei Key Laboratory of Advanced Memories, Hubei Engineering Research Center on Microelectronics, Huazhong University of Science and Technology, Wuhan 430074, China

[2]Hubei Yangtze Memory Laboratories, Wuhan 430205, China

[3] Wuhan Xinxin Semiconductor Manufacturing Corporation, Wuhan, 430205, China

*Authors to whom correspondence should be addressed: shj@hust.edu.cn;

S1 Device Forming voltage comparison diagram

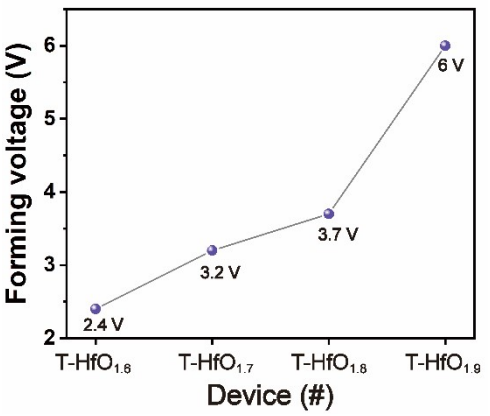

Fig.S1. Comparison diagram of Forming voltage values of four devices

As shown in Fig.S1, the Forming voltage of T-$HfO_{1.6}$ is 2.4 V, that of T-$HfO_{1.7}$ is 3.2 V, that of T-$HfO_{1.8}$ is 3.7 V, and that of T-$HfO_{1.9}$ is 6 V. It can be seen that the Forming voltage increases with the increase of x value.

S2 Comparison diagram of low resistance consistency of T-$HfO_{1.7}$ with other memristor devices

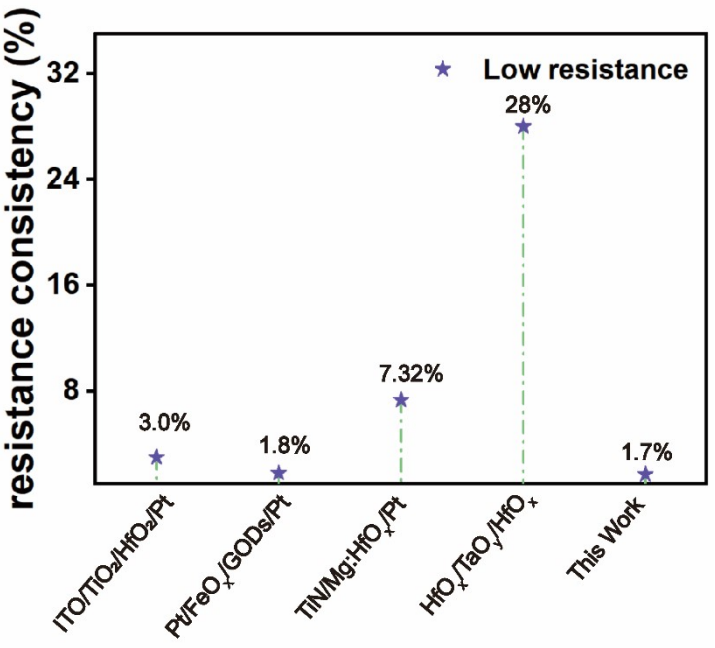

Fig.S2. Low resistance consistency comparison diagram

As shown in Fig. S2, comparing T-$HfO_{1.7}$ with other memristor devices[1-4] with improved consistency, T-$HfO_{1.7}$ has good low-resistance consistency because we control the CFs breakage in the HfO_2 middle layer.

S3 Pavlov's dog experiment of T-$HfO_{1.7}$ device

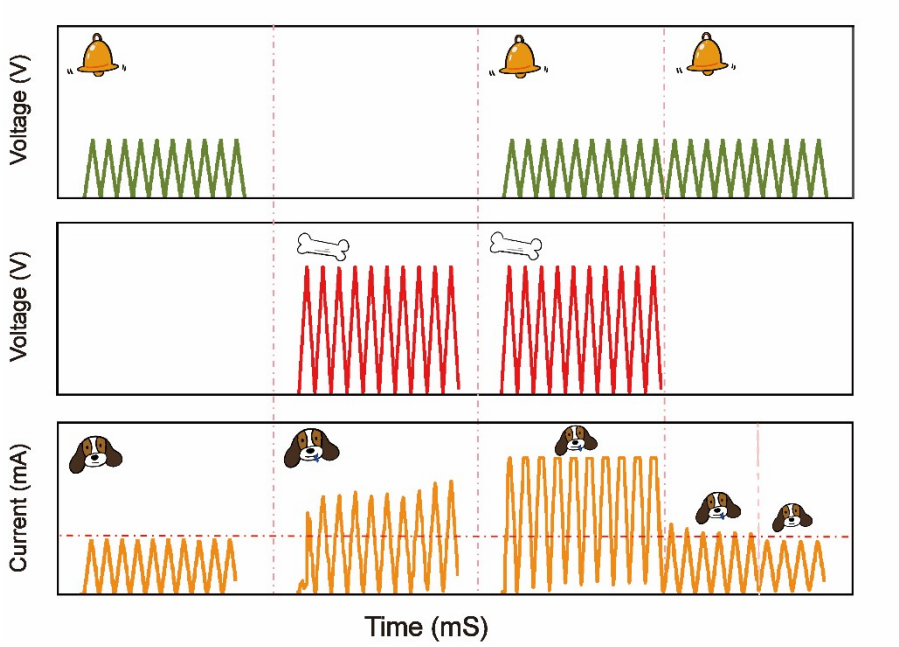

Fig.S3. Device implementation of Pavlov's dog process diagram

As shown in Fig. S3, first, a single bell ringing does not cause the dog to salivate, the T-$HfO_{1.7}$ is placed in a low conduction state, and the pulse stimulation with an amplitude of 1V is used to simulate the bell ringing, and the T-$HfO_{1.7}$ is still in a low conduction state. The food alone causes the dog to salivate, and a pulse stimulus with a amplitude of 3V is used to simulate the food, which can be seen to put the T-$HfO_{1.7}$ in a high conduction state; Further, in the training process, the dog was fed when the bell rang, establishing a connection between the food and the bell, after this training, when the food was removed, the bell sounded, the dog would also secrete saliva, and voltage was applied to the T-$HfO_{1.7}$ at the same time. It can be observed that when the 3V pulse stimulation was removed, the device was still in a high conductivity state, but with the increase of time, after the food was removed, the T-$HfO_{1.7}$ was still in a high conductivity state. The association between food and ringing gradually weakens and disappears.

S3 Estimation of non-ideal factors

The mathematical fitting of T-$HfO_{1.7}$'s simulated weight update behavior is as follows[5]：

$$G_{LTP} = B\left(1 - e^{\frac{-N}{A}}\right) + G_{min} \#(1.1)$$

$$G_{LTD} = G_{max} - B\left(1 - e^{\frac{N - N_{max}}{A}}\right) \#(1.2)$$

$$B = \left(G_{max} - G_{min}\right) / \left(1 - e^{\frac{-N_{max}}{A}}\right) \#(1.3)$$

Where G_{LTP} and G_{LTD} are functions of the LTP/LTD curve varying with the number of pulses N, G_{max} and N_{max} is the saturation conductance value and the maximum number of pulses allowed to be applied, respectively, and A and B are the parameters to be fitted. Further, the nonlinearity (α)can be fitted:

$$\alpha = \frac{1.726}{A + 0.162} \#(1.4)$$

Table S1. CV of LRS, HRS and Nonlinear parameter of LTD/LTP between synaptic memristor devices

Device	CV of LRS/HRS	Nonlinear parameter of LTP/LTD	Ref.
$Au/HfO_x/TaO_y/HfO_x/Ti/TiN$	0.28/0.57	5.3/11.9	4
Pt/HfO_2 NRs/TiN	0.219/0.312		6
$Pt/TiO_x/ZnO/SiO_2/TaN$	0.155/0.326	8/0.52	7
Al/A-C-B-D TiO_x/Al		2.4/4.6	8
$n\text{-}Si/HfO_2/WO_3/Ag$		2.49/5.54	9
$T\text{-}HfO_{1.7}$	0.017/0.126	1.55/4.55	This work

References

1. L.-H. Li, K.-H. Xue, L.-Q. Zou, J.-H. Yuan, H. Sun and X. Miao, *Appl. Phys. Lett.*, 2021, 119.
2. R. Zhang, H. Huang, Q. Xia, C. Ye, X. Wei, J. Wang, L. Zhang and L. Q. Zhu, *Adv. Electron. Mater.*, 2019, 5.
3. C. Wang, W. He, Y. Tong, Y. Zhang, K. Huang, L. Song, S. Zhong, R. Ganeshkumar and R. Zhao, *Small*, 2017, 13.
4. D. Sakellaropoulos, P. Bousoulas, G. Nikas, C. Arvanitis, E. Bagakis and D. Tsoukalas, *Microelectron. Eng.*, 2020, 229.
5. Y. Fu, B. Dong, W. C. Su, C. Y. Lin, K. J. Zhou, T. C. Chang, F. Zhuge, Y. Li, Y. He, B. Gao and X. S. Miao, *Nanoscale*, 2020, 12, 22970-22977.
6. J. U. Kwon, Y. G. Song, J. E. Kim, S. Y. Chun, G. H. Kim, G. Noh, J. Y. Kwak, S. Hur, C.-Y. Kang, D. S. Jeong, S. J. Oh and J. H. Yoon, *ACS Appl. Mater. Interfaces*, 2022, 14, 44550-44560.
7. M. Ismail, M. Rasheed, C. Mahata, M. Kang and S. Kim, *J. Alloys Compd.*, 2023, 960, 170846.
8. M. Kim, K. Yoo, S. P. Jeon, S. K. Park and Y. H. Kim, *Micromachines (Basel)*, 2020, 11.
9. Q. Liu, S. Gao, Y. Li, W. Yue, C. Zhang, H. Kan and G. Shen, *Adv. Mater. Technol.*, 2023, 8, 2201143.